Electronic Supplementary Material (ESI) for Chemical Communications.
This journal is © The Royal Society of Chemistry 2022

Electronic Supporting Information File:

Mechanistic Insight into Rapid Oxygen-Atom Transfer from a Calix-Functionalized Polyoxovanadate

Alex A. Fertig, Shannon E. Cooney, Rachel M. Meyer, William W. Brennessel, and Ellen M. Matson*

Department of Chemistry, University of Rochester, Rochester, New York 14627, United States

Supporting Information Table of Contents:

Experimental.

General Considerations. All manipulations were carried out in the absence of water and oxygen using standard Schlenk techniques, or in a UniLab MBraun inert atmosphere drybox under a nitrogen atmosphere. All glassware was oven-dried for a minimum of 3 hours and cooled in an evacuated antechamber prior to use in the drybox. All solvents were dried and deoxygenated on a Glass Contour System (Pure Process Technology, LLC) and stored over activated 4 Å molecular sieves purchased from Fisher Scientific prior to use. 3 Å molecular sieves purchased from Fisher Scientific were activated in a Schlenk flask for at least 48 hours at 125 ºC under vacuum prior to use. Anhydrous methanol (99.8%) was purchased from Sigma-Aldrich and stored over activated 3 Å molecular sieves in a nitrogen filled glove box. Triethylamine was dried and distilled over calcium hydride and stored over 3 Å molecular sieves in a nitrogen filled glovebox. Silver trifluoromethanesulfonate, tetrabutylammonium borohydride, and Dimethylphenylphosphine was purchased from Sigma Aldrich and used as received. $V_6O_7(OMe)_{12}$, $V_6O_6(OMe)_{12}OPMe_2Ph$, 4-t-Butylcalix[4]arene, $HNEt_3[(calix)V_6O_6(OMe)_8]$, and $[(calix)V_6O_6(OMe)_8]$ were prepared according to published procedures.[1-5]

^{1}H NMR spectra were recorded at 500 MHz on a Bruker DPX-500 MHz spectrometer locked on the signal of deuterated solvents. All chemical shifts were reported relative to the peak of residual H signal in deuterated solvents. THF-d_8 was purchased from Cambridge Isotope Laboratories and stored in the drybox over activated 4Å molecular sieves. Infrared (FT-IR, ATR) spectra of complexes were recorded on a Shimadzu IRAffinity-1 Fourier Transform Infrared Spectrophotometer and are reported in wavenumbers (cm^{-1}). Electronic absorption measurements were recorded at room temperature in anhydrous acetonitrile in a sealed 1 cm quartz cuvette with an Agilent Cary 60 UV-Vis spectrophotometer. Elemental analyses were performed on a PerkinElmer 2400 Series II Analyzer, at the Elemental Analysis Facility located at the University of Rochester.

Single crystals of $[(calix)V_6O_7(OMe)_8]$ and $[(calix)V_6O_6(OPMe_2Ph)(OMe)_8]$ were mounted on the tip of a thin glass optical fiber (goniometer head) and mounted on a XtaLab Synergy-S Dualflex diffractometer equipped with a HyPix-6000HE HPC area detector for data collection at 100.00(10)-192.99(10) K, respectively. The structure was solved using SHELXT-2018/2[7] and refined using SHELXL-2018/3.[8]

Synthesis of $[(calix)V_6O_7(OMe)_8]$ (2). A 20 mL scintillation vial was charged with $[(calix)V_6O_6(OMe)_8(MeCN)]$ (0.058 g, 0.0437 mmol) and 6 mL dichloromethane (DCM). Iodosobenzene (0.014 g, 0.063 mmol) was added as a solid with stirring. The reaction was stirred at 45 °C for 2 hours, whereupon a green solution formed. The crude solid was dried under reduced pressure and collected by extraction in diethylether (Et_2O), filtered over celite. The solid was dried in vacuo to give $[(calix)V_6O_7(OMe)_8]$ (0.056 g, 0.0427 mmol, 97%). Crystalline material was obtained by creating a concentrated solution of the product in acetonitrile (MeCN), and allowing the solvent to slowly evaporate at room temperature over the course of several days. ^{1}H NMR (400 MHz, $CDCl_3$): d = 33.90, 15.55, 8.60, 8.00, 4.93, 1.23. FT-IR (ATR,cm^{-1}): 1030 (O_b-CH_3), 986 (V=O_t). UV-Vis (THF): 1000 (ε = 1163), 400 (sh, ε = 4028), 316 (ε = 10184). Elemental analysis: Calc. for $C_{52}H_{76}O_{19}V_6$ • ½ Et_2O (MW = 1347.9 g/mol): C, 48.12; H, 6.06. Found: C, 47.8; H, 5.9; N, 0.18.

Synthesis of $[(calix)V_6O_7(OPMe_2Ph)(OMe)_8]$ (2-$OPMe_2Ph$). A 20 mL scintillation vial was charged with $[(calix)V_6O_7(OMe)_8]$ (0.1314 g, 0.1002 mmol) and 6 mL tetrahydrofuran (THF). Dimethylphenylphosphine (0.0195 g, 0.1102 mmol) was added with stirring. The reaction was stirred at 40 °C for 1 hour, whereupon a brown solution formed. The crude product was dried under reduced pressure and was washed with n-pentane (2 mL x 3), filtered over celite to collect the brown precipitate. The solid was extracted in DCM and dried in vacuo to give $[(calix)V_6O_7(OMe)_8PMe_2Ph]$ (0.0658 g,

0.0448 mmol, 45%). Crystalline material was obtained by creating a concentrated solution of the product in $CDCl_3$ and allowing the solvent to slowly evaporate off over the course of a couple days. ^{1}H NMR (400 MHz, $CDCl_3$): d = 33.22, 30.08, 29.11, 8.24, 8.06, 4.93, 1.66, 1.10. FT-IR (ATR,cm^{-1}): 1045 (O_b-CH_3), 987 (V=O_t), 1157 (P=O). UV-Vis (THF): 1000 (ε = 512), 314 (sh, ε = 9413). Elemental analysis: Calc. for $C_{60}H_{87}O_{19}PV_6$ • 1 MeCN 1½ $CDCl_3$ (MW = 1669.07 g/mol): C, 45.7; H, 5.53; N, 0.84. Found: C, 45.39; H, 5.91; N, 0.64.

General Procedure for performing Pseudo-first Order Reaction Kinetics. For all kinetic experiments, concentration of cluster in solution was determined by comparing the relative integration of the target cluster in solution against 2 mM of the internal standard, Hexamethyldisiloxane (HMDS). Calibration curves were obtained by collecting ^{1}H NMR spectra of the desired cluster in solution at a range of concentrations (0.5 – 10 mM cluster) with 2 mM of HMDS present. Plotting relative integration against the concentration of cluster in solution will produce a linear trend, with which the concentration of cluster in solution can be calculated.

Pseudo-First order reaction conditions were used in order to establish the rate expression for the reaction between the POV-alkoxide clusters **2** and $[V_6O_7(OMe)_{12}]$ and dimethylphenylphosphine (PMe_2Ph). In order to determine the order of each reactant with respect to the rate expression, the initial rate of the reaction was measured using ^{1}H NMR spectroscopy, where the concentration of the respective cluster can be measured over time. To find the order with respect to **2**, a 0.1 mL sample of Tetrahydrofuran-d_8 (THF-d_8) containing 840 mM of PMe_2Ph and 8 mM HMDS as an internal standard was prepared in a J-Young tube. The sample was then frozen using liquid nitrogen, and an aliquot of a stock solution of THF-d_8 containing the cluster **2** (21.33 mM stock solution) was added and kept frozen. If needed, additional THF-d_8 was then added to reach a final volume of 0.4 mL. Once frozen, the sample was quickly transferred to the spectrometer set to the desired temperature. A ^{1}H NMR spectrum was then collected every 10 seconds for 15 minutes in order to collect the initial rate of reaction. Once completed, the reaction was repeated using a different concentration of **2**.

In order to find the order with respect to PMe_2Ph in the reaction with **2**, a 0.4 mL sample of THF-d_8 containing 15 mM of **2** and 8 mM HMDS as an internal standard was prepared in a J-Young tube. The sample was then frozen using liquid nitrogen, and an aliquot of a stock solution of THF-d_8 containing PMe_2Ph (88 mM stock solution) was added and kept frozen. If needed, additional THF-d_8 was then added to reach a final volume of 0.4 mL. Once frozen, the sample was quickly transferred to the spectrometer set to the desired temperature. A ^{1}H NMR spectrum was then collected every 10 seconds for 15 minutes in order to collect the initial rate of reaction. Once completed, the reaction was repeated using a different concentration of PMe_2Ph.

In order to establish the order with respect to $[V_6O_7(OMe)_{12}]$, a 0.3 mL sample of THF-d_8 containing 840 mM of PMe_2Ph and 8 mM HMDS as an internal standard was prepared in a J-Young tube. The sample was then frozen using liquid nitrogen, and an aliquot of a stock solution of THF-d_8 containing the cluster $[V_6O_7(OMe)_{12}]$ (21.33 mM stock solution) was added and kept frozen. If needed, additional THF-d_8 was then added to reach a final volume of 0.4 mL. Once frozen, the sample was quickly transferred to the spectrometer set to 21° C, and an initial ^{1}H NMR spectrum was collected. The J-Young tube was then placed into a water bath set to a desired temperature and allowed to sit. ^{1}H NMR spectra were collected periodically over 24 hours, where the sample would be removed from the water bath and chilled in an ice bath in order to halt the reaction. After the ^{1}H NMR spectrum was collected, the sample would be placed back into the water bath until the next time point.

In order to find the order with respect to PMe_2Ph in the reaction with $[V_6O_7(OMe)_{12}]$, a 0.4 mL sample of THF-d_8 containing 15 mM of $[V_6O_7(OMe)_{12}]$ and 0.8 mM HMDS as an internal standard was prepared in a J-Young tube. The sample was then frozen using liquid nitrogen, and an aliquot of a stock solution of THF-d_8 containing PMe_2Ph (88 mM stock solution) was added and kept frozen. If needed, additional THF-d_8 was then added to reach a final volume of 0.4 mL. Once frozen, the sample was

quickly transferred to the spectrometer set to 21°, and an initial ^{1}H NMR spectrum was collected. The J-Young tube was then placed into a water bath set to a desired temperature and allowed to sit. ^{1}H NMR spectra were collected periodically over 24 hours, where the sample would be removed from the water bath and chilled in an ice bath in order to halt the reaction. After the ^{1}H NMR spectrum was collected, the sample would be placed back into the water bath until the next time point.

General Procedure for Determining Activation Energy for OAT. Activation parameters were determined using kinetic data obtained by measuring the initial rate of change in concentration of cluster in solution, over a range of temperatures. Pseudo-first order reaction conditions were utilized in order to simplify determining the observed rate constants for each temperature, where the concentration of PMe_2Ph was held in excess over the cluster. From the results collected in the variable temperature experiments, the activation parameters are able to be established using the linear form of the Eyring-Polanyi equation, shown in Eqn 1,

$$\ln\left(\frac{k}{T}\right) = -\frac{\Delta H^{\ddagger}}{R} * \frac{1}{T} + \ln\left(\frac{k_B}{H}\right) + \frac{\Delta S^{\ddagger}}{R} \qquad \text{Eqn 1}$$

$$\Delta G^{\ddagger} = \Delta H^{\ddagger} - T\Delta S^{\ddagger} \qquad \text{Eqn 2}$$

Where T is the temperature, $\Delta H^{\ddagger}$ is the enthalpy of activation, $\Delta S^{\ddagger}$ is the entropy of activation, R is the universal gas constant (R = 1.987x^{-3} kcal K^{-1} mol^{-1}), k_B is the Boltzmann constant, and h is Planck's constant. The rate constant k is found by dividing the observed rate constant found in the pseudo-first order conditions, by the concentration of the phosphine in solution. Plotting ln(k/T) vs. 1/T gives a plot with a linear best fit line, from which the enthalpy of activation can be found by slope = $-\Delta H^{\ddagger}/R$. In addition, the entropy of activation can be found from the y-intercept, where y-intercept =ln (k_B/h) + $\Delta S^{\ddagger}/R$. From these parameters, the activation free energy can be determined at the desired temperature using Eqn 2. All values are reported at 95% confidence interval by linear regression using Excel.

Table S1: Crystallographic parameters for molecular structures of complexes **1**, **2**, and **2-OPMe$_2$Ph**.

Compound	**1**	**2**	**2-OPMe$_2$Ph**
Empirical formula	$C_{54}H_{79}NO_{18}V_6$	$C_{62}H_{91}N_5O_9V_6$	$C_{63.17}H_{94.09}N_{0.42}O_{19.59}PV_6$
Formula weight	1335.82	1516.03	1509.26
Temperature / K	100.00(10)	99.99(10)	100.00(10)
Wavelength / Å	1.54184	1.54184	1.54184
Crystal group	Monoclinic	Monoclinic	Orthorhombic
Space group	*I*2/a	*I*2/a	*Pnma*
Unit cell dimensions	*a* =20.0174(2) Å *b* =17.51540(10) Å *c* =21.2630(2) Å α = 90° β = 104.9550(10)° γ = 90°	*a* =21.2605(2) Å *b* =17.61780(10) Å *c* =20.1094(2) Å α = 90° β = 104.8300(10)° γ = 90°	*a* =22.5148(4) Å *b* =20.0029(3) Å *c* =15.83572(19)Å α = 90° β = 90° γ = 90°
Volume / Å^3	7202.57(11)	7281.34(11)	7131.78(17)
Z	4	4	4
Reflections collected	46776	46057	48193
Independent reflections	7578	7666	7723
Completeness (theta)	99.8% (74.504°)	99.7% (74.504°)	99.9% (74.504°)
Goodness-of-fit on F^2	1.067	1.080	1.093
Final *R* indices [*I*>2sigma(*I*)]	*R*1 = 0.0366	*R*1 = 0.0428	*R*1 = 0.0587
Largest diff. peak and hole (e.Å^{-3})	0.400 and -0.512	0.671 and -0.849	0.733 and -0.608

Table S2. Bond valence sum calculations for crystallographically independent vanadium ions in **1** based on X-ray crystallographic data collected at 100 K. Table reflects the results of BVS calculations using V-O bond valence parameters (r_0) for different oxidation states of vanadium.

2	V1	V2	V3	V4
V(III)	3.0739	3.6144	3.6109	4.2399
V(IV)	3.4342	**4.0380**	**4.0341**	4.7367
V(V)	3.6151	4.2508	4.2466	**4.9863**

Table S3. Bond valence sum calculations for crystallographically independent vanadium ions in **2** based on X-ray crystallographic data collected at 100 K. Table reflects the results of BVS calculations using V-O bond valence parameters (r_0) for different oxidation states of vanadium.

2	V1	V2	V3	V4
V(III)	4.1471	3.6325	3.1900	4.2276
V(IV)	4.6440	**4.0581**	**3.5638**	4.7230
V(V)	**4.8771**	4.2720	3.715	**4.9718**

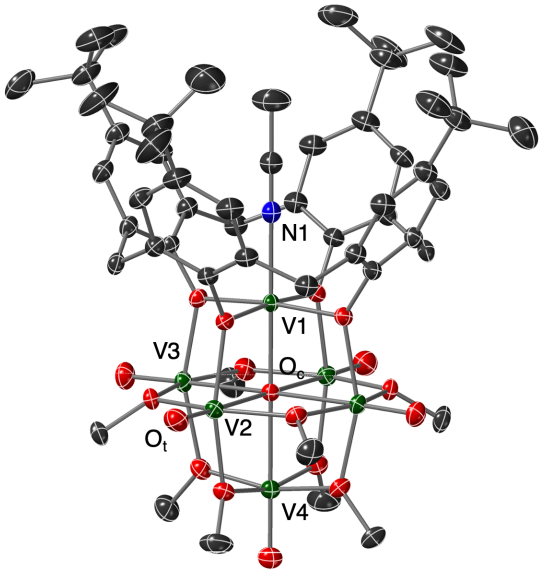

Figure S1. Molecular structure of **1** shown with 30% probability ellipsoids. Hydrogen atoms and co-crystallized solvent molecules have been removed for clarity. Key: V, dark green; O, red; C, grey; N, blue.

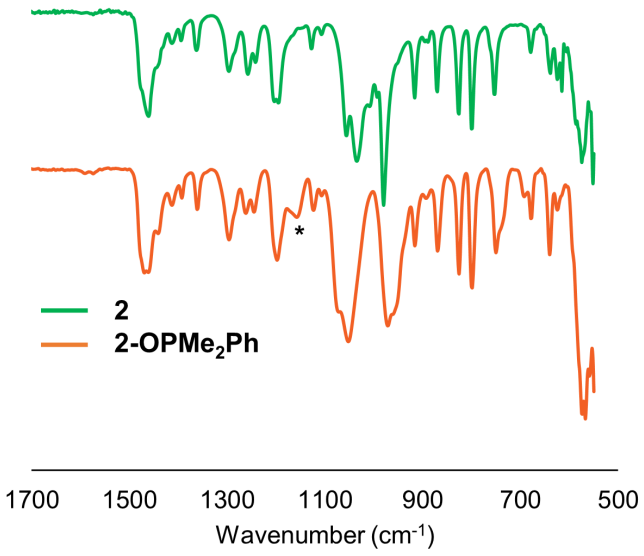

Figure S2. FT-IR spectra of the clusters **2** (green, top) and **2-OPMe$_2$Ph** (orange, bottom). Stretching frequency characteristic of (O=P) functional groups is marked with *, indicating the formation the phosphine bound cluster, **2-OPMe$_2$Ph**.

Table S4. Key stretching frequencies of **2** and **2-OPMe$_2$Ph**.

	2	**2-OPMe$_2$Ph**
$\nu(O_b\text{-}C_2H_5)$	1030 cm^{-1}	1045 cm^{-1}
$\nu(V{=}O_t)$	986 cm^{-1}	987 cm^{-1}
$\nu(O{=}P)$	---	1157 cm^{-1}

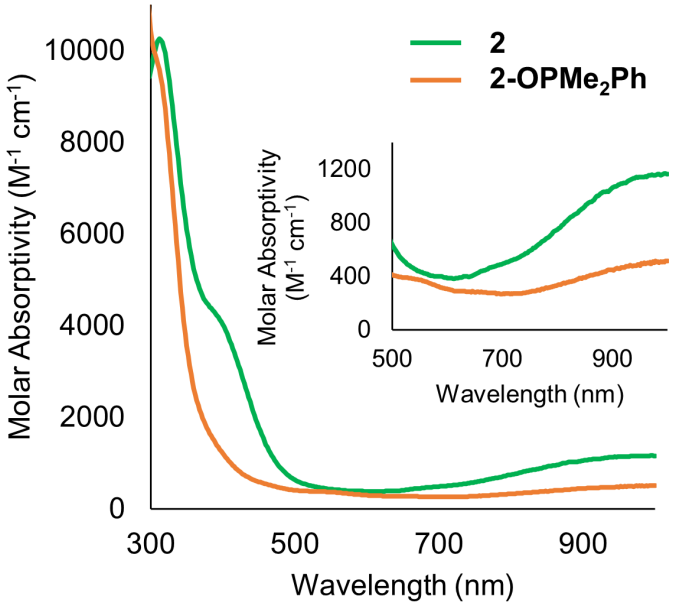

Figure S3. Electronic absorption spectra of **2** (green) and **2-OPMe$_2$Ph** (orange). Results were collected at 21 ºC in THF.

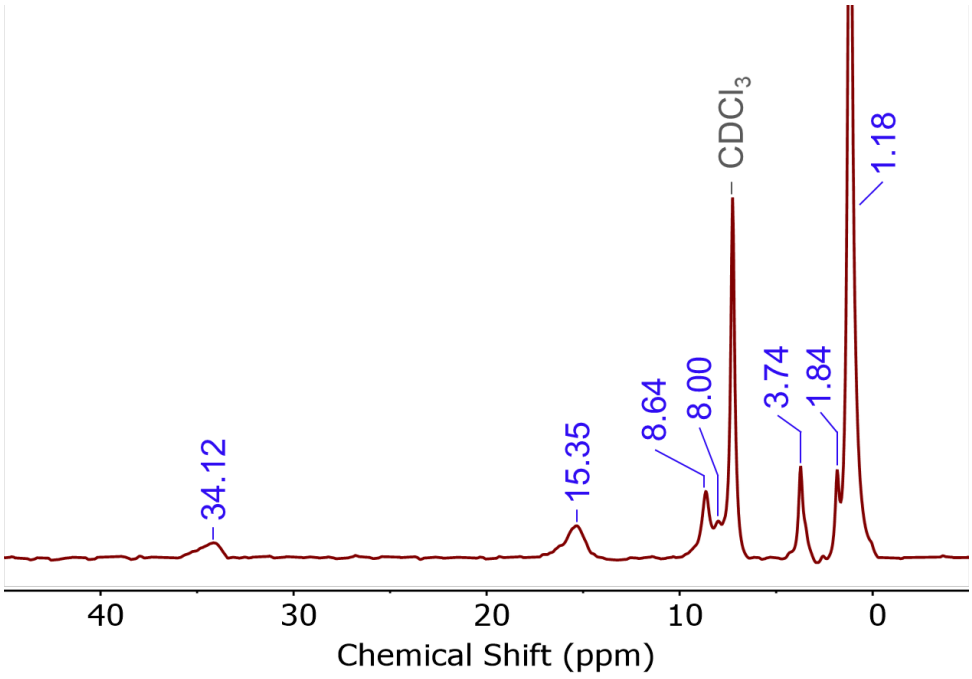

Figure S4. ^{1}H NMR spectrum of **2**, collected in $CDCl_3$ at 21 °C.

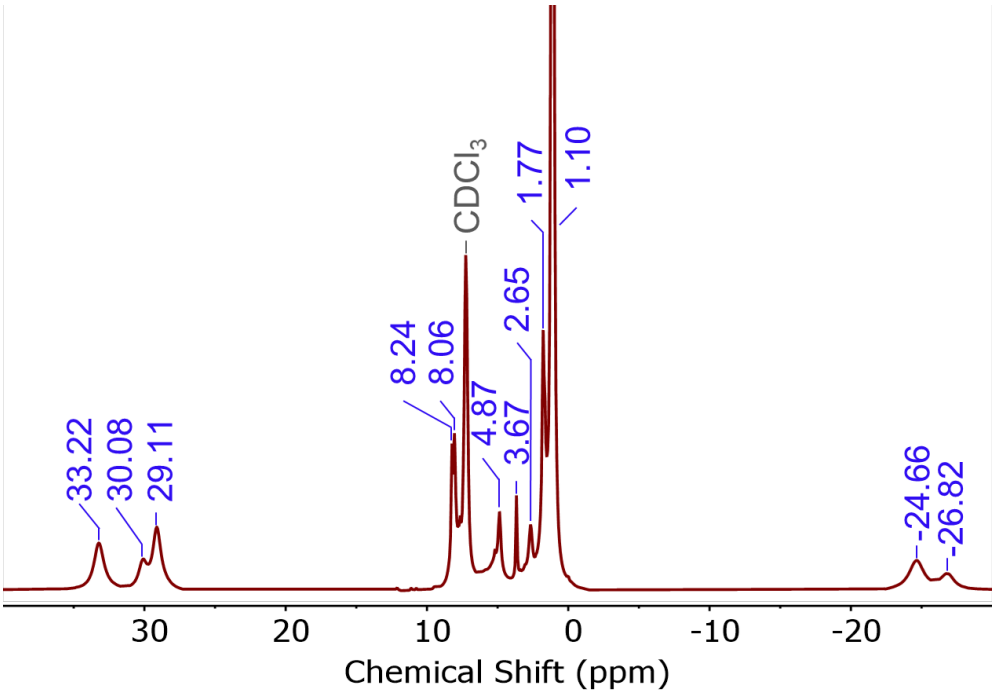

Figure S5. ^{1}H NMR spectrum of **2-OPMe$_2$Ph**, collected in $CDCl_3$ at 21 °C. The 5 paramagnetically shifted signals belong to the 5 chemically distinct bridging alkoxide ligands found at the surface of the cluster. Upon addition of the PMe_2Ph, the cluster undergoes a loss of symmetry to C_S. This results in 3 pairs of chemically identical bridging methoxide ligands, in addition to two distinct bridging methoxide ligands, resulting in 5 paramagnetically shifted signals

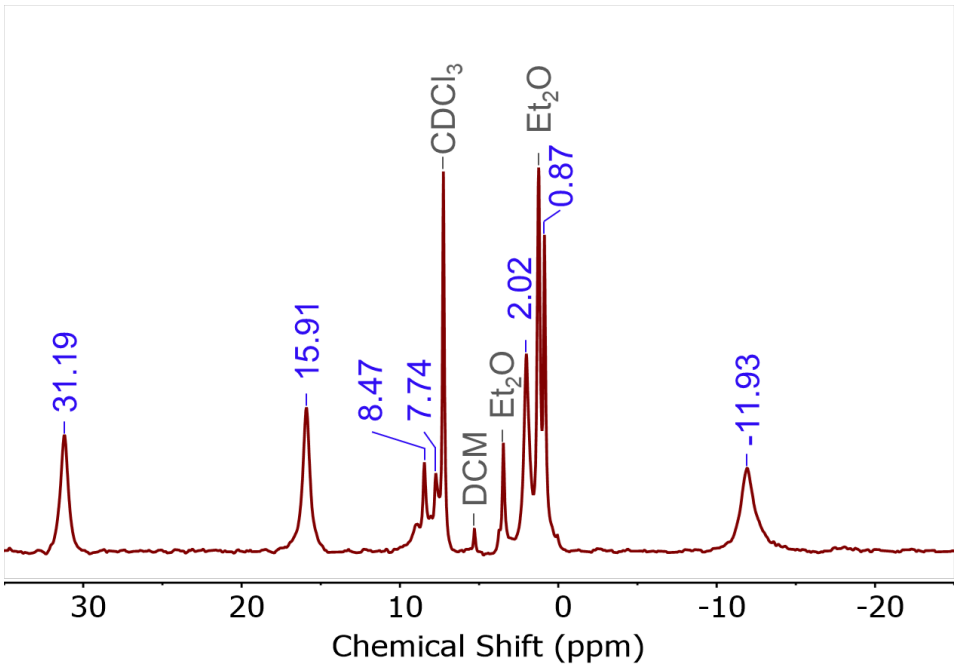

Figure S6. ^{1}H NMR spectrum of $[V_6O_6(OMe)_{12}OPMe_2Ph]$, collected in $CDCl_3$ at 21 °C.

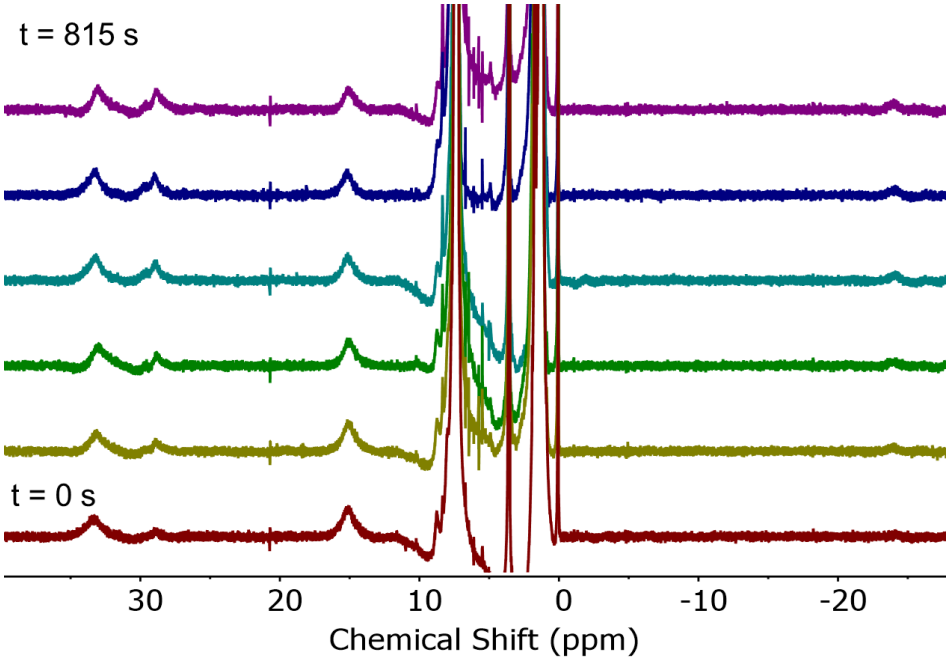

Figure S7. ^{1}H NMR spectra collected at various time points for the reaction between **2** and PMe_2Ph. The reaction was run with 2 mM of HMDS as an internal standard in THF-d_8 at room temperature. As the reaction progresses, the appearance of signals at 29.1 and -24 ppm indicates the formation of the product, **2-OPMe$_2$Ph**. Initial rate of reaction was found by measuring the change in concentration of the initial cluster, **2**, as a function of time.

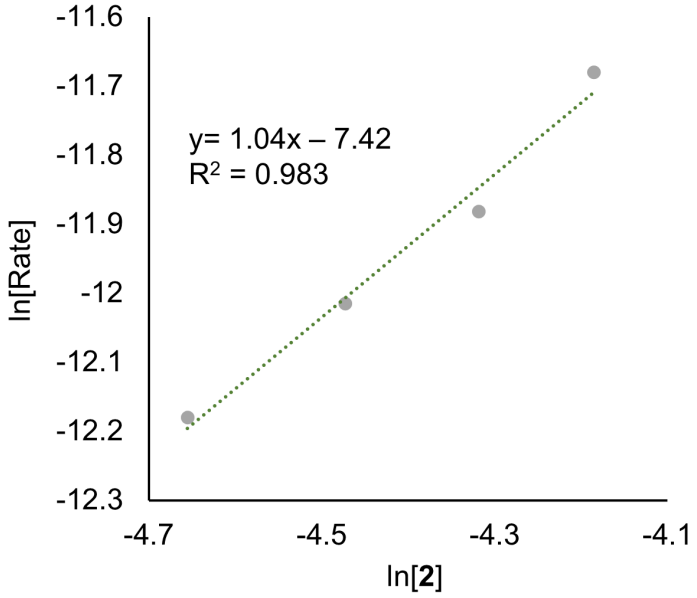

Figure S8. Plot to determine the order with respect to **2** in the reaction between **2** and PMe_2Ph. The concentration of PMe_2Ph was held in excess relative to the concentration of the cluster, allowing for pseudo-first order reaction kinetics to be used. Each data point represents the natural log of the initial rate of reaction against the natural log of the concentration of cluster initially in solution. The approximate slope of 1 indicates an order of one with respect to the cluster. All results were collected by measuring rate of the disappearance of the initial cluster, **2**, using ^{1}H NMR spectroscopy at 25 °C.

Table S5. Tabulated results for the experiments to determine the order with respect to **2** in the reaction between **2** and PMe_2Ph. Values from this table are used to create the plot found in Figure S8. Each reaction was run at room temperature in THF-d_8 with 2 mM HMDS as an internal standard.

[PMe2Ph] (M)	[**2**] (M)	ln[**2**]	Initial Rate (M/s)	ln(Initial Rate)
0.21	0.01	-4.60	5.12×10^{-6}	-12.18
0.21	0.012	-4.42	6.04×10^{-6}	-12.01
0.21	0.014	-4.26	6.92×10^{-6}	-11.88
0.21	0.016	-4.13	8.46×10^{-6}	-11.68

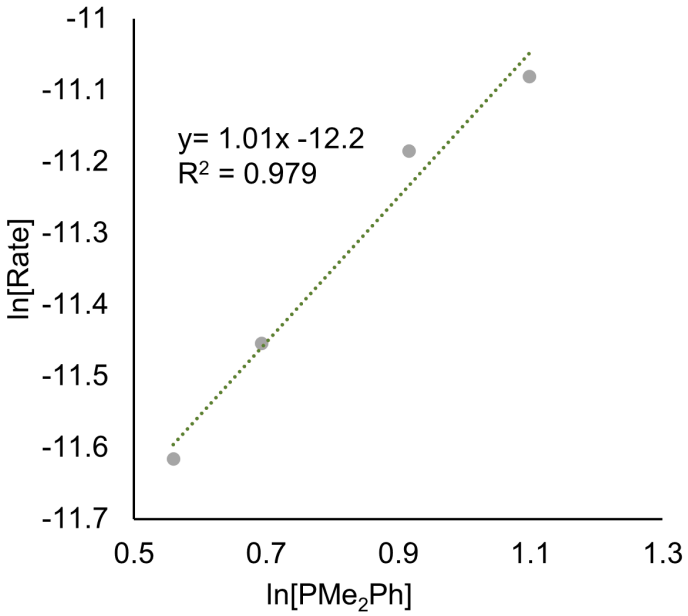

Figure S9. Plot to determine the order with respect to PMe_2Ph in the reaction between **2** and PMe_2Ph. The concentration of **2** was held in excess relative to the concentration of the phosphine, allowing for pseudo-first order reaction kinetics to be used. Each data point represents the natural log of the initial rate of reaction against the natural log of the concentration of phosphine initially in solution. The approximate slope of 1 indicates an order of one with respect to PMe_2Ph. All results were collected by measuring rate of the disappearance of the initial cluster, **2**, using ^1H NMR spectroscopy at 25 °C.

Table S6. Tabulated results for the experiments to determine the order with respect to PMe_2Ph in the reaction between **2** and PMe_2Ph. Values from this table are used to create the plot found in Figure S8. Each reaction was run at room temperature in THF-d_8 with 2 mM HMDS as an internal standard.

[PMe_2Ph] (M)	ln(PMe_2Ph)	**2** (M)	Initial Rate (M/s)	ln(Initial Rate)
0.00175	0.0159	9.02×10^{-6}	-6.34	-11.61
0.002	0.0159	1.06×10^{-5}	-6.21	-11.45
0.0025	0.0159	1.38×10^{-5}	-5.99	-11.18
0.003	0.0159	1.54×10^{-5}	-5.81	-11.08

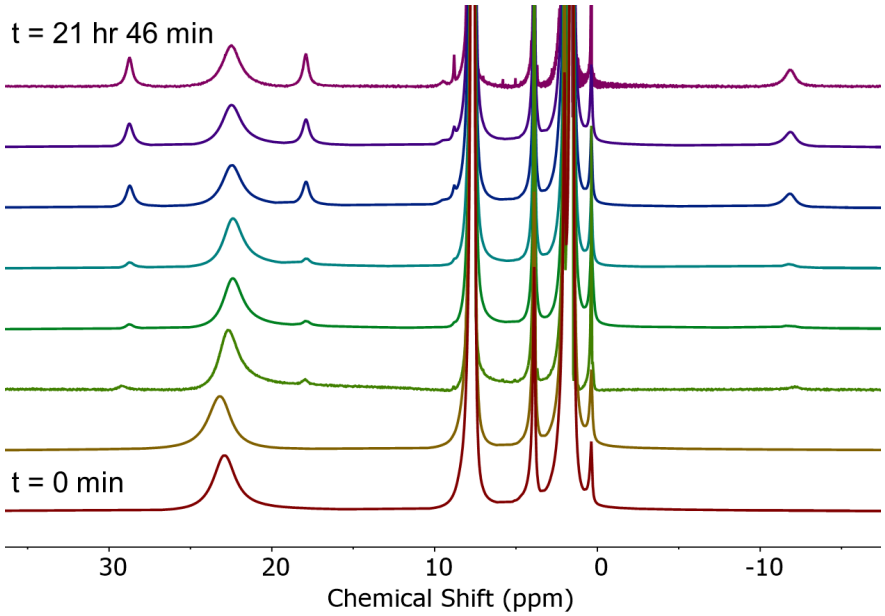

Figure S10. ^{1}H NMR spectra collected at various time points for the reaction between $V_6O_7(OMe)_{12}$ and PMe_2Ph. The reaction was run with 2 mM of HMDS as an internal standard in THF-d_8 at room temperature. As the reaction progresses, the gradual disappearance of the signal at 22.9 ppm, belonging to $V_6O_7(OMe)_{12}$, is accompanied by the appearance of a three peak pattern indicating formation of product cluster, $[V_6O_6(OMe)_{12}OPMe_2Ph]$. Initial rate of reaction was found by measuring the change in concentration of the product cluster, $[V_6O_6(OMe)_{12}OPMe_2Ph]$, as a function of time.

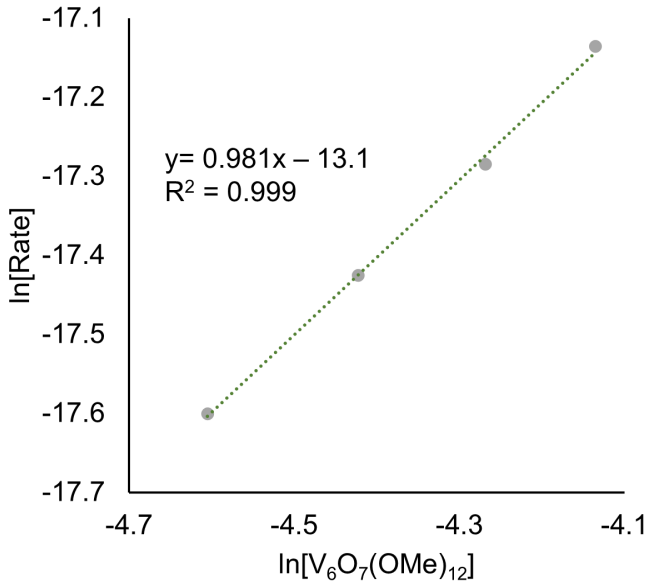

Figure S11. Plot to determine the order with respect to $V_6O_7(OMe)_{12}$ in the reaction between $V_6O_7(OMe)_{12}$ and PMe_2Ph. The concentration of PMe_2Ph was held in excess relative to the concentration of the cluster, allowing for pseudo-first order reaction kinetics to be used. Each data point represents the natural log of the initial rate of reaction against the natural log of the concentration of cluster initially in solution. The approximate slope of 1 indicates an order of one with respect to the cluster. All results were collected by measuring rate of the appearance of the product cluster, $[V_6O_6(OMe)_{12}OPMe_2Ph]$, using ^{1}H NMR spectroscopy at 25 °C.

Table S7. Tabulated results for the experiments to determine the order with respect to $V_6O_7(OMe)_{12}$ in the reaction between $V_6O_7(OMe)_{12}$ and PMe_2Ph. Values from this table are used to create the plot found in Figure S11. Each reaction was run at room temperature in THF-d_8 with 2 mM HMDS as an internal standard.

[PMe_2Ph] (M)	[$V_6O_7(OMe)_{12}$] (M)	ln[$V_6O_7(OMe)_{12}$]	Initial rate (M/s)	ln(Initial rate)
0.21	0.01	-4.60	2.27×10^{-8}	-17.60
0.21	0.012	-4.42	2.70×10^{-8}	-17.42
0.21	0.014	-4.26	3.11×10^{-8}	-17.28
0.21	0.016	-4.13	3.61×10^{-8}	-17.13

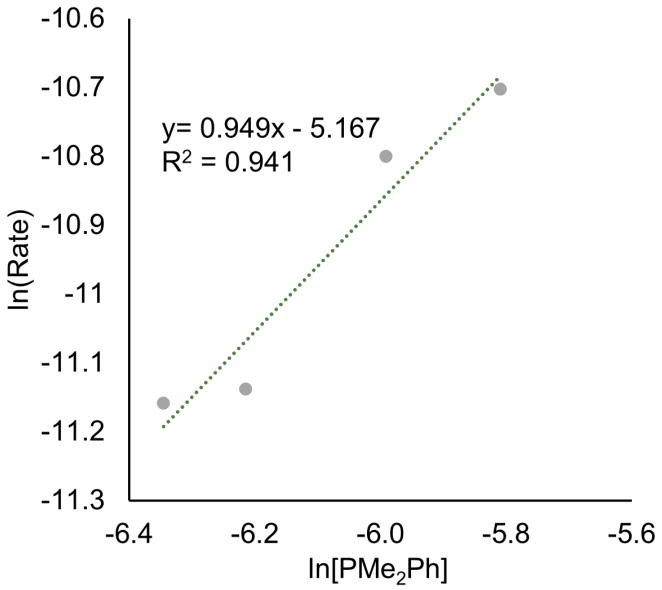

Figure S12. Plot to determine the order with respect to PMe_2Ph in the reaction between $V_6O_7(OMe)_{12}$ and PMe_2Ph. The concentration of $V_6O_7(OMe)_{12}$ was held in excess relative to the concentration of the cluster, allowing for pseudo-first order reaction kinetics to be used. Each data point represents the natural log of the initial rate of reaction against the natural log of the concentration of phosphine initially in solution. The approximate slope of 1 indicates an order of one with respect to PMe_2Ph. All results were collected by measuring rate of the appearance of the product, $[V_6O_6(OMe)_{12}OPMe_2Ph]$, using ^1H NMR spectroscopy at 25 °C.

Table S8. Tabulated results for the experiments to determine the order with respect to PMe_2Ph in the reaction between $V_6O_7(OMe)_{12}$ and PMe_2Ph. Values from this table are used to create the plot found in Figure S12. Each reaction was run at room temperature in THF-d_8 with 2 mM HMDS as an internal standard.

$[PMe_2Ph]$ (M)	$\ln[PMe_2Ph]$	$[V_6O_7(OMe)_{12}]$ (M)	Initial rate (M/s)	ln(Initial Rate)
0.00175	-6.35	0.015	1.42×10^{-5}	-11.16
0.002	-6.21	0.015	1.45×10^{-5}	-11.14
0.0025	-5.99	0.015	2.04×10^{-5}	-10.8
0.003	-5.81	0.015	2.24×10^{-5}	-10.7

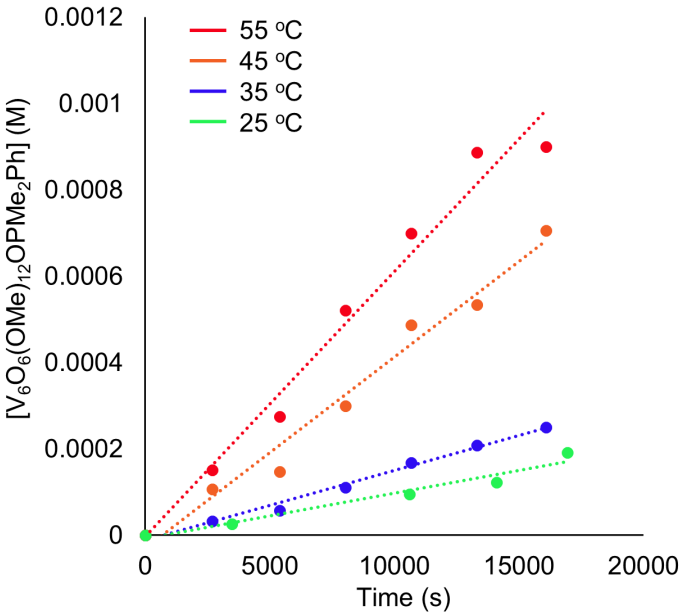

Figure S13. Initial rates of reaction between $V_6O_7(OMe)_{12}$ and PMe_2Ph at various temperatures. Results are determined by measuring the concentration of the product, $[V_6O_6(OMe)_{12}OPMe_2Ph]$, as a function of time. Concentrations are determined by ^1H NMR spectroscopy in d_8-THF.

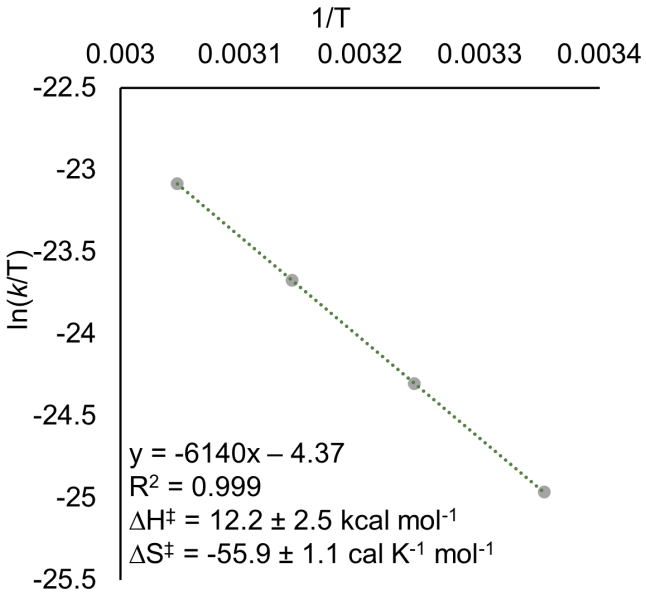

Figure S14. Results of Eying analysis for the reaction of $V_6O_7(OMe)_{12}$ and PMe_2Ph. Experiments were conducted at temperatures ranging from 25 to 55 °C. At each temperature interval, experiments were repeated in order to ensure accuracy in results. All results were collected by measuring rate of appearance of the product, $[V_6O_6(OMe)_{12}OPMe_2Ph]$, using ^1H NMR spectroscopy.

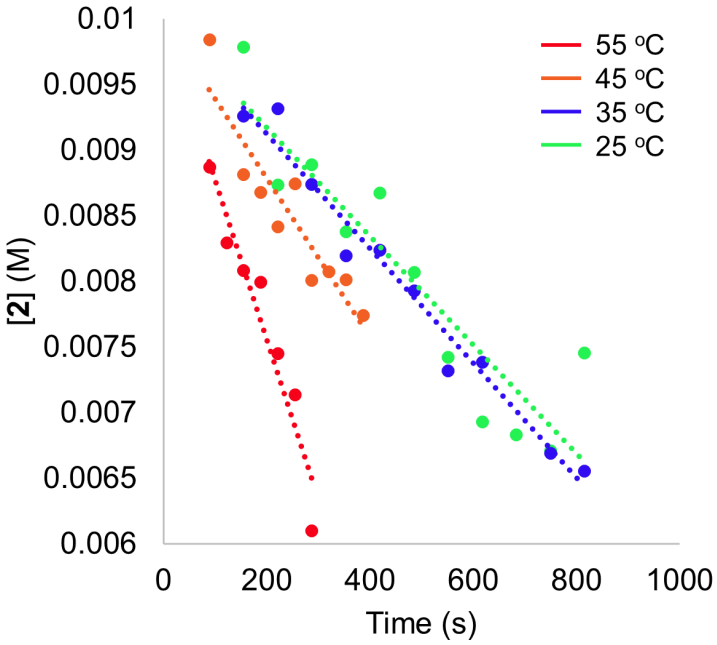

Figure S15. Comparison of the initial rates of reaction between **2** and PMe_2Ph at various temperatures. Results are plotted as concentrtaion of the parent cluster, **2**, as a function of time. Initial concentration of **2** in each experiemnt is 10 mM. Concentrations are determined by ^1H NMR spectroscopy in d_8-THF.

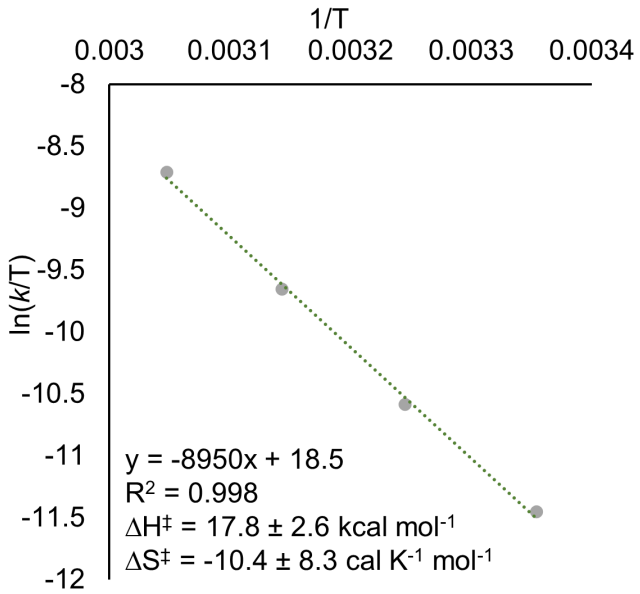

Figure S16. Results of Eying analysis for the reaction of **2** and PMe_2Ph. Experiments were conducted at temperatures ranging from 25 to 55 °C. At each temperature interval, experiments were repeated in order to ensure accuracy in results. All results were collected by measuring rate of disappearance of the reactant, $[(calix)V_6O_7]$, using ^1H NMR spectroscopy.

References:

1. J. Spandl, C. Daniel, I. Brüdgam and H. Hartl, *Angew. Chem. Int. Ed.*, 2003, **42**, 1163-1166.
2. C. Daniel and H. Hartl, *J. Am. Chem. Soc.*, 2005, **127**, 13978-13987.
3. C. Aronica, G. Chastanet, E. Zueva, S. A. Borshch, J. M. Clemente-Juan and D. Luneau, *J. Am. Chem. Soc.*, 2008, **130**, 2365-2371.
4. C. D. Gutsche and M. Iqbal, *Org. Synth.*, 1990, **68**.
5. B. E. Petel, R. L. Meyer, W. W. Brennessel and E. M. Matson, *Chem. Sci.,* 2019, **10**, 8035-8045.
6. R. L. Meyer, P. Miro, W. W. Brennessel, E. M. Matson, *Inorg. Chem.,* 2021, **60**, 13833-13843.
7. G. M. Sheldrick, *Acta Crystallogr., Sect. A*, 2015, **71**, 3-8.
8. G. M. Sheldrick, *Acta Crystallogr., Sect. C*, 2015, **71**, 3-8.